

The anomalous merging of the African and North Atlantic
jet streams during Northern Hemisphere winter of 2010. *

N. Harnik

Department of Geophysical, Atmospheric and Planetary Sciences,

Tel-Aviv University, Israel

E. Galanti

Department of Geophysical, Atmospheric and Planetary Sciences,

Tel-Aviv University, Israel

O. Martius

Institute of Geography and Oeschger Centre for Climate Change Research

University of Bern, Bern, Switzerland

O. Adam

Department of Earth Sciences, ETH Zurich, Switzerland

April 9, 2014

Abstract

The North Atlantic jet stream during winter 2010 was unusually zonal, so that the typically separated Atlantic and African jets were merged into one zonal jet. Moreover, the latitude-height structure and temporal variability of the North Atlantic jet during this winter were more characteristic of the North Pacific. This work examines the possibility of a flow regime change, from an eddy-driven to a mixed eddy/thermally-driven jet. A monthly jet zonality index is defined, which shows that a persistent merged jet state has occurred in the past at the end of the 1960s, and during a few sporadic months. The anomalously zonal jet is found to be associated with anomalous tropical Pacific diabatic heating and eddy anomalies similar to those found during a negative NAO state. A Lagrangian back trajectory diagnosis of eight winters suggests the tropical Pacific is indeed a source of momentum to the African jet, and that this source was stronger during the winter or 2010. The results suggest that the combination of weak eddy variance and fluxes in the North Atlantic, along with strong tropical heating, act to push the jet towards a merged eddy/thermally-driven state. We also find significant SST anomalies in the North Atlantic, which reinforce the anomalous zonal winds, in particular in the Eastern Atlantic.

*Corresponding author address: Nili Harnik, Department of Geophysics and Planetary Sciences, Tel-Aviv University, Israel. Email: harnik@tau.ac.il

17 1 Introduction

18 One of the main characteristics of the midlatitude atmospheric flow is its organization into zonally
19 oriented jet streams. Meteorologists have long noticed two types of jet streams- subtropical
20 jets which form due to meridional advection of angular momentum by the Hadley cells (e.g.
21 Schneider, 1977; Held and Hou, 1980), and polar front jets, also referred to as eddy-driven
22 jets, which form due to the convergence of momentum by baroclinically unstable eddies as they
23 propagate away from their source region (e.g. Held, 1975; Rhines, 1975; Panetta, 1993; Held,
24 2000). noted that these processes force both jets simultaneously, but under certain forcing
25 conditions eddy generation is close enough to the subtropical jet so that a single merged jet
26 evolves (see also O'Rourke and Vallis, 2013). Son and Lee (2005) further showed that a merged
27 jet forms preferentially when the tropical heating is strong enough for the resultant subtropical
28 jet to influence the growth of midlatitudes eddies, while a double jet forms when tropical heating
29 is weak enough to allow mid-latitude eddies to grow more poleward and form a separate eddy-
30 driven jet. The type of jet stream strongly affects the weather and correspondingly the climate
31 in a given region. Eichelberger and Hartmann (2007) showed that the different jet types have
32 very different temporal variability. While eddy-driven jets tend to meander latitudinally, due
33 to the nature of wave-mean flow feedbacks, the thermally-driven or merged jets hardly shift in
34 latitude and instead their variability is associated more with a pulsation of the jet.

35 While the above studies were all tested using models with zonally symmetric surface con-
36 ditions, the main jet categorization and implied jet characteristics seem to apply to the real
37 atmosphere when considering specific zonal sectors. In particular, the North Pacific jet has a
38 vertical structure and temporal variability characteristic of a merged thermally/eddy-driven jet
39 while the North Atlantic jet is eddy-driven, and it coexists with a subtropical jet which starts
40 over the Eastern Atlantic and extends over Africa and Asia (e.g. Son and Lee, 2005; Eichelberger

41 and Hartmann, 2007). Recently, Li and Wettstein (2012) explicitly showed in reanalysis data
42 that the Atlantic jet is mostly eddy-driven, while the Pacific jet is both thermally-driven and
43 eddy-driven.

44 In models, the transition from a single to a double jet occurs quite abruptly when external
45 forcing parameters are gradually varied (e.g. Lee and Kim, 2003; Son and Lee, 2005). In particu-
46 lar, in Son and Lee (2005) the jet changed from an eddy driven state to a merged eddy-thermally
47 driven state when the tropical forcing was strengthened or the midlatitude baroclinicity weak-
48 ened. Recently, Lachmy and Harnik (2014) showed that the important factor by which the
49 midlatitude baroclinicity affects the jet stream type is the strength of the eddies. Moreover, a
50 change in jet type can be induced by changing eddy damping while keeping the mean flow forcing
51 fixed.

52 In the real atmosphere, jet type transitions have been noted to occur as part of the seasonal
53 cycle, and might occur in the future as the climate changes (e.g. Son and Lee, 2005). It is possible
54 that such changes may also occur inter-annually, in response, for example, to the regular inter-
55 annual variability in tropical heating. Indeed, an examination of the inter-annual variability
56 in the Atlantic jet structure suggests that during some years, a single rather than double jet
57 forms (Woollings et al., 2010b). Most striking is the winter of 2010 (hereafter, winter refers to
58 Dec-Mar months with the year referring to Jan-Mar), which exhibited an unusually strong and
59 persistent negative phase of the North Atlantic Oscillation and unusually cold and wet conditions
60 over North America and Europe (Wang et al., 2010; Seager et al., 2010; Cattiaux et al., 2010;
61 Vincente-Serrano et al., 2011; Santos et al., 2013). As shown below, during this winter, the
62 Atlantic and African jets merged into one zonally oriented jet, with structure and variability
63 more characteristic of the Pacific.

64 In this study we propose that while the NAO phases are a manifestation of the eddy-driven jet

65 meandering in latitude, some of the extremely negative NAO winters correspond to a change in
66 the type of jet stream, from an eddy-driven jet to a mixed thermally/eddy-driven jet, as is found
67 in the Pacific. We will show that besides negative NAO conditions, a weakening of midlatitude
68 eddies as well as anomalously strong tropical diabatic heating were involved. After presenting
69 the data and analysis methods (Sec. 2), we characterize the anomalous conditions of the Atlantic
70 jet during the winter of 2010, define an appropriate index to identify other months during which
71 the jet was unusually zonal, and show that indeed during such winter months the Atlantic and
72 African jets merged (Section 3). We then examine the change in eddy and thermal driving (Secs.
73 4.1 and 4.2 respectively), and the possible role of the ocean, given large sea surface temperature
74 (SST) anomalies in the Atlantic and Pacific (Sec. 5). In Sec. 6 we examine the relation between
75 jet zonality and different atmospheric indices. We conclude with a discussion in Sec. 7.

76 **2 Data and analysis methods**

77 For much of the analysis we use daily and monthly mean wind and temperature fields from NCEP
78 re-analysis data for 1949-2012 (Kalnay et al., 1996) (the results were unchanged when using 1958-
79 2012). For some of the eddy diagnostics, in particular a Lagrangian trajectory analysis, we used
80 the ECMWF ERA40 (Uppala et al., 2005) and ERA Interim (Dee et al., 2011) data sets. To
81 examine thermal forcing we use NCEP and ERA Interim radiative and sensible heat fluxes and
82 precipitation, to calculate total atmospheric column diabatic heating. We also use precipitation
83 rates from the Global Precipitation Climatology Project (GPCP) version 2.2 (Adler et al., 2003),
84 which is the combined precipitation data developed and computed by the NASA/Goddard Space
85 Flight Center’s Laboratory for Atmospheres as a contribution to the GEWEX Global Precipi-
86 tation Climatology Project. We note that NCEP radiative fluxes only exist since 2002, while

87 ERA Interim and GPCP data sets start in 1979. We used the NOAA Climate Prediction Center
88 (CPC) North Atlantic Oscillation (NAO) index (based on the method developed by Barnston,
89 1987) and the Nino3.4 index, calculated by CPC from the NCDC Extended Reconstructed Sea
90 Surface Temperature (ERSST, Smith and Reynolds, 2004; Smith and Lawrimore, 2008). The
91 ERSST data was also used to examine Atlantic sea surface temperatures.

92 To study the contribution and influence on synoptic scale eddies we divide the main daily
93 mean NCEP fields into short and long time scales, using a simple top-hat filter with a cutoff
94 of 10 days, so that eddies are defined as the 10 day high pass filtered data, while the mean
95 flow is defined as the 10 day low passed filtered data. We then calculate eddy fluxes as the low
96 passed covariances between high-passed fields. Examining meridional wind variances using a 24
97 hour difference filter which spans 2-8 day periods gave similar results. A Lagrangian analysis of
98 the momentum sources of the jets in the Atlantic basin and over Africa is done by calculating
99 back-trajectories up to one week back (see Martius and Wernli, 2012, and Martius, 2014, for
100 details). To examine possible causes and effects of an anomalously zonal jet state, we calculate
101 composites of various fields, by averaging monthly data over subsets of the Dec-Mar winter
102 months. Statistical significance is calculated from the anomaly field composites using a standard
103 two-sided T-test against climatology, with anomaly defined as the deviation from a monthly
104 climatological seasonal cycle. Regions for which the anomalies are significant are shaded, both
105 on plots of the full field and of anomaly field composites. Unless otherwise noted, the results we
106 present will be from NCEP reanalysis, for the years 1949-2012, but we verified that the main
107 features of the composite analyses hold also for ERA40 and ERA Interim.

108 **3 The unusually zonal Atlantic-African jet state**

109 **3.1 The anomalous conditions during winter 2010**

110 One of the anomalous features of the Northern winter 2010 in the Atlantic, which has not
111 received much attention so far, is the merging of the Atlantic and African jets. Fig 1 shows the
112 upper and lower level jet during this winter, alongside climatological winds. For this part of the
113 analysis we use daily and monthly mean winds from NCEP re-analysis, for 1949-2012 (Kalnay
114 et al., 1996). We see that during 2010 the Atlantic jet became zonally oriented, while the
115 African jet shifted a bit poleward, so that the two jets merged into one. An examination of the
116 latitude-height structure of the Atlantic jet during this winter, in comparison to the climatological
117 Atlantic and Pacific jets (Fig. 2) shows more similarity to the Pacific which has a single jet with
118 strong baroclinic and barotropic components. Consistent with Eichelberger and Hartmann (2007)
119 the anomalous jet configuration during this winter was unusually persistent, and its temporal
120 variability was more characteristic of the jet variability in the Pacific than in the Atlantic (Fig. 3).

121 **3.2 The Zonal Jet Index (ZJI)**

122 The main feature which characterizes the merged Atlantic and African jets is their unusual
123 zonality. We therefore define a Zonal Jet Index (ZJI), which will allow us to objectively identify
124 other such periods. Looking at the 300 *hPa* zonal wind field (we used either monthly or seasonal
125 averages), we first find the latitude of the jet axis ($\varphi_{ja}(\lambda)$), defined at each longitude λ as the
126 latitude φ with maximum zonal wind values (thick black lines in Fig. 1), and calculate its zonal
127 derivative ($\frac{d\varphi_{ja}}{d\lambda}$). This derivative will have the largest magnitude (large negative values) at the
128 point where the jet axis jumps from the Atlantic to the African jet. During years when the
129 jet is very zonal, as in Figure 1a, this gradient will be small (in absolute value) everywhere.

130 Using the monthly or seasonal averaged winds, we calculate the maximum absolute value of the
131 zonal gradient of the latitude of the jet axis, and define the ZJI as the monthly anomaly of this
132 quantity from its climatological seasonal cycle. Defined this way, the ZJI will be anomalously
133 negative during months with an unusually zonal jet. Fig. 4a shows the corresponding ZJI time
134 series using monthly mean zonal mean winds at 300 *hPa*. The figure shows all months, but we
135 marked with solid dots those Dec-Mar months for which the ZJI anomaly (of both signs) exceeds
136 one standard deviation (dashed lines). Note that anomalously zonal jet configurations (negative
137 ZJI anomaly) have occurred during all seasons but we only concentrate on winter months. We
138 see that the ZJI during the winter of 2010 is negative and anomalously persistent, with all 4
139 winter months being strongly negative. This is highlighted when we examine the ZJI calculated
140 from the Dec-Mar mean 300 *hPa* zonal wind (Fig. 4b). We also see that there are other months
141 and winters with a negative ZJI index, with more such months occurring in the earlier half of
142 the time series, and other very anomalous ZJI winters occurring only prior to 1971.

143 **3.3 The characteristic negative ZJI jet structure**

144 Figure 5a shows a composite of monthly mean 300 *hPa* winds for winter months with strongly
145 negative ZJI values, based on a 1 standard deviation threshold (the dots below the lower dashed
146 line in Fig. 4a). We see that indeed during months with anomalously negative ZJI values the
147 Atlantic and African jets merged to one unusually zonal jet. The corresponding zonal wind
148 anomaly composite (Fig. 5b), plotted along with the composite jet axis (thick black line) show
149 an equatorward shift of the Atlantic jet, and a poleward shift of the jet over eastern-central Africa.
150 In contrast, the composite for anomalously positive ZJI (the dots above the upper dashed line in
151 Fig. 4a), shown in Fig. 5c, shows a strongly slanted Atlantic jet which is well separated from the
152 African jet, but the pattern is not statistically significant. This is due to the large variability in

153 split-jet structures, which partly reflects the trimodal structure of the distribution of Atlantic jet
154 latitudes (Woollings et al., 2010a). Also shown, for reference, is the corresponding composite for
155 negative NAO months (based on 1 standard deviation, Fig. 5d). We see that while the Atlantic
156 jet is similar between the negative NAO and negative ZJI composites, the African jet does not
157 shift poleward as much for the negative NAO, so that the two jets are not connected as in the
158 winter of 2010. In what follows we only examine the negative ZJI state, and note that the
159 index was only tested for the monthly and winter mean Atlantic-African jets, so that it does not
160 necessarily work as an indication of jet merging in other regions and on other time scales.

161 **4 Dynamical characteristics of anomalously zonal jet months**

162 In this section we examine the characteristics of various circulation features during months with
163 an unusual zonal Atlantic jet configuration, with the aim of understanding what drove the jet to
164 shift to a merged state and what maintains it. In particular, we examine changes in eddy and
165 thermal driving, and how they related to the changes in the mean flow. We start by calculating
166 negative ZJI composites of various fields. These composites consist of averaging monthly data
167 over those Dec-Mar months for which the ZJI index is negative by more than 1 standard deviation
168 (the dots below the lower dashed line in Fig. 4a).

169 **4.1 Eddy driving**

170 One of the main sources of variance to the Atlantic jet structure is a change in the synoptic scale
171 eddies, which nonlinearly interact with the jet. Fig. 6a-c shows the negative ZJI composites
172 of eddy meridional wind variance, chosen to represent the midlatitude storm track, alongside
173 its climatological field. As expected, the storm track is more zonally oriented during zonal jet

174 years, with its eastern edge reaching Spain rather than Great Britain. Apart for an equatorward
175 shift, however, the eddies weaken during zonal jet years (this is despite the ZJI composite being
176 an average over much fewer months than climatology). This is most evident from the anomaly
177 composite (Fig. 6c). This overall weakening is also evident in the anomalous eddy heat and
178 momentum fluxes (Fig. 6d,e). While in the climatology, the eddy heat fluxes are mostly positive
179 and assume the North-Eastward slant of the Atlantic jet, during zonal jet months, the eddy
180 heat flux anomaly (Fig. 6d) is mostly negative over the central and Eastern North Atlantic
181 and positive over Europe, suggesting eddy growth is greatly suppressed but extends further
182 eastwards, consistent with less efficient baroclinic growth in a more zonal storm track. Eddy
183 momentum fluxes, which are typically directed polewards over most of the storm track region,
184 are significantly weaker during zonal jet years (Fig. 6e), with small increases in the subtropics
185 over the Eastern Atlantic and Africa, due to the equatorwards shift of the eddies. This decrease
186 results in an anomalous eddy momentum flux convergence (Fig. 6f) which accelerates the flow
187 south of $40^{\circ}N$ and decelerates it poleward of $40^{\circ}N$, reinforcing the observed zonal wind anomaly
188 (Fig. 4b)¹.

189 It is important to note that the analysis presented shows instantaneous effects, indicating con-
190 sistency, and not causality. We do not expect to be able to establish causality from observations
191 since the eddies and the jet feedback on each other and the time scales are sub monthly. The
192 above results are however consistent with a transition to a merged jet state, as follows. In the
193 eddy-driven jet regime, the tropical thermally-driven direct mean meridional circulation which
194 continuously forces westerly winds at the subtropics is weak, so that the eddy momentum flux
195 convergence dominates and forces a jet in midlatitudes. When the midlatitude eddies and their

¹We also examined the contribution of zonal momentum flux convergence and found it to be negligible compared to the meridional component.

196 associated eddy momentum flux convergence are weaker, as is observed to be the case during
197 zonal jet years, the thermal driving of the jet can play a more significant role. The equilibrated
198 jet in this case is more equatorward and is affected by both thermal and eddy driving (c.f. Son
199 and Lee, 2005; Lachmy and Harnik, 2014). At the same time, the transition to a merged jet state
200 will also weaken eddy amplitudes, by trapping the upper level disturbances equatorwards of the
201 latitude of strongest surface baroclinicity and making baroclinic growth less efficient (Nakamura
202 and Sampe, 2002).

203 **4.2 Thermal driving**

204 Son and Lee (2005) showed that stronger tropical heating leads to a single merged jet, while
205 weaker heating leads to a strong eddy-driven jet alongside a weaker subtropical jet. Li and
206 Wettstein (2012) examined observed monthly mean Northern Hemisphere winter data and showed
207 that in the Pacific, monthly variations in the jet stream correlated strongly both with midlatitude
208 eddy momentum flux convergence and with various proxies of thermal driving. In the Atlantic, on
209 the other hand, they found a strong correlation only with the eddy momentum flux convergence.
210 Given the similarity between the Atlantic and Pacific jets during negative ZJI months, we expect
211 thermal driving to play a larger role during such months. Following Li and Wettstein (2012)
212 we use total column integrated diabatic heating calculated directly from the monthly reanalyses
213 products by summing the net short and long wave radiative fluxes into the atmospheric column
214 (top of atmosphere and surface fluxes), the surface vertical sensible heat flux, and the latent heat
215 released by local precipitation (Eq. 5 of Trenberth and Solomon, 1994). Since radiation data in
216 NCEP reanalysis are only given since 1992, we also use ERA Interim, which starts in 1979.

217 Fig. 7a,b shows the negative ZJI monthly anomaly composites for both reanalyses. We see
218 a significant Atlantic tripole pattern, with anomalous heating over the midlatitude Atlantic, a

219 large negative anomaly in the northern part of the Atlantic just south of Greenland, and a weak
220 anomalous diabatic cooling in the subtropical Atlantic, which is stronger in NCEP than in ERA
221 Interim, similar to what is found for a negative NAO. In the tropics, however, we do not see a
222 significant signal over the Atlantic, but we do see significant anomalous heating in the equatorial
223 Pacific. These anomalies are consistent with El Nino conditions, which were observed during
224 winter 2010. These results suggest that anomalous tropical Pacific heating forces a stronger
225 Atlantic subtropical jet, strong enough to cause it to transition from a double to a single jet
226 during these months. This is actually consistent with Fig. 2 of Li and Wettstein (2012) which
227 shows a zonal wind anomaly in the mid-latitude Atlantic in composites of extreme tropical Pacific
228 diabatic heating, but not in composites of tropical Atlantic diabatic heating.

229 Since latent heat release is a major component of the diabatic heating fields (e.g. Romanski,
230 2013), but this field is highly dependent on the analysis model parameterizations, we also examine
231 monthly GPCP precipitation fields (Adler et al., 2003). The precipitation rate ZJI anomaly,
232 shown in Fig. 7c, looks quite similar to the diabatic heating anomalies, though there is no clear
233 negative anomaly in the subtropical Atlantic, and the positive midlatitude anomaly is only over
234 the Eastern half of the Atlantic. As with diabatic heating, there is a significant positive anomaly
235 over the Central and Eastern Pacific, and even a hint of a midlatitude Eastern Pacific dipole.

236 We note, from Fig. 4, that a significant number of the negative ZJI months occurred prior
237 to 1979, thus the diabatic heating and precipitation composites consist of only 10 negative ZJI
238 months after 2002, and 3 more between 1979-2001. To extend the composite analysis back in
239 time and include the zonal jet months prior to 1979, we examine vertical pressure velocity (ω)
240 using NCEP reanalysis for the period 1949-2012. As was shown, for example by Li and Wettstein
241 (2012), the climatological ω pattern captures the diabatic heating and precipitation fields well.
242 The negative ZJI ω anomaly composite is shown in Fig. 7d. For clarity, we plot negative values

(upward motion) which indicate diabatic heating, in solid. We see anomalous ascent over the tropical Pacific, and a tripole anomaly pattern over the Atlantic. As with the precipitation anomalies, the significant midlatitude ascent occurs only over the Eastern half of the Atlantic. To examine causality, we calculate time lagged composites of all the above fields. Fig. 7e shows a composite of the ω field 2 months prior to the anomalously negative ZJI months. We see a significant tropical Pacific anomaly (with the anomaly starting to be significant already in month -3 , not shown), suggesting the Tropical Pacific heating at least partially drives the anomalous jet state. The time lead of tropical Pacific heating is also evident from the SST anomalies which at time lag of -2 months (Fig. 7f) show a very clear positive anomaly which is maximal in the central tropical Pacific, and consistent with El Nino conditions. This tropical Pacific anomaly develops as early as 3 months before the jet becomes zonal, and diminishes only after the peak negative ZJI month (not shown).

The El Nino conditions during winter 2010 prompted Santos et al. (2013) to examine the role of the tropical Pacific in forcing the variability of the Atlantic jet. They did not, however, find a significant signal, suggesting this was a coincidence which occurred during winter 2010. To further verify the robustness of our results, we repeated the composite calculations using subsets of the data. Figure 8a shows the composite of ω anomalies at 0 time lag, for 1949-2011 excluding the four winter months of winter 2010. We see significant ascent in the tropical Pacific (with anomalies being significant as early as month -3), suggesting the tropical Pacific forcing is not unique to winter 2010. We also repeat the analysis for 1979-2012 (Fig 8b,c), and find much weaker anomalies with no significant signal when we remove the winter 2010 months, similar to Santos et al. (2013) (who used ERA interim from 1979). To more closely examine the monthly signals, we define a Tropical Pacific Ascent Index (TPAI) as the average of ω (weighted by cosine latitude) in a tropical box extending from $200^{\circ}W - 100^{\circ}W$, $15^{\circ}S - 15^{\circ}N$ (marked

267 in blue on Fig. 8a), and plot it against the monthly Dec-Mar ZJI time series, with the winter
268 months up to 1978 in red and the rest in blue. For reference, we mark the line of -1 ZJI standard
269 deviation, and mark the 2010 winter months by large circles. We see that about two thirds of the
270 negative ZJI months also have negative TPAI values (anomalous ascent), with more negative ZJI
271 months with negative TPAI before 1979. The winters of 2010, 1970, 1969 and 1958, which had
272 a negative ZJI for a few consecutive months (Fig. 4), had anomalously negative TPAI values.
273 Overall, the results support our notion that the tropical Pacific contributes to the anomalous
274 merging of the Atlantic and African jets during a few very anomalous months.

275 To further examine the role of tropical Pacific heating on the Atlantic jets, we use a back
276 trajectory calculation similar to Martius and Wernli (2012) and Martius (2014). The subtropical
277 jet is forced to first order by the export of angular momentum from the tropics into the subtropics.
278 The angular momentum is modulated in the subtropics by eddies. However, the role of the eddies
279 is of secondary importance during the winter (e.g. Bordoni and Schneider, 2010; Martius, 2014).
280 The back trajectories thus indicate where the transport of angular momentum from the tropics
281 into the subtropics happens. Here we use this analysis to examine the tropical Pacific contribution
282 to air flowing into the Atlantic jet entrance ($90^{\circ}W - 45^{\circ}W$) and African jet ($30^{\circ}W - 30^{\circ}E$) regions.
283 Since the analysis is very computationally intensive, it has only been carried out for 8 winters
284 (Dec-Feb, year corresponding to Jan-Feb), using ERA Interim. Based on Fig 4b, we chose 1996,
285 2005 and 2010 as representative negative ZJI winters, while 1997 and 2006-2009, which were not
286 negative ZJI years, were chosen for comparison. For each day during a given winter, the back
287 trajectory calculation first picks the grid points which constitute the jet, based on characteristics
288 of a subtropical jet - wind velocities above $40m/sec$ and the vertical shear concentrated at upper-
289 levels (see Koch et al., 2006). These grid points serve as starting points for the back-trajectory
290 calculation which is run for 7 days (168 hours). Fig. 9 shows the fraction of the total number of

trajectories which cross each grid point over the entire seven day period, as well as the region from which the calculation is started (thick black contour), calculated for the negative ZJI winters of 1996, 2005 and 2010, and an average over 5 other winters (1997, 2006-2009). Also shown is the difference between the two plots. During the years when the jet has a more typical structure, the air parcels that end up in the wintertime subtropical jet over Africa typically ascend into the upper troposphere and hence enter the northward directed branch of the Hadley cell over South America (Martius, 2014). During the negative ZJI winters, a smaller than usual fraction of trajectories reached the subtropical jet over Africa and the Atlantic from South America. In contrast an anomalously large fraction of the air parcels moved northwards from the equator into the subtropics from the tropical Pacific, in particular over the Eastern part ($120^{\circ}W - 90^{\circ}W$)². In addition, more air flows into the jet from the subtropics, consistent with a strongly zonal flow, and less comes from mid latitudes, South America, or the Tropical Atlantic. The African jet also shows a greater contribution from far upstream sources (Asia and the Pacific and even the eastern subtropical Atlantic), compared to closer upstream air (the western subtropical Atlantic) during the negative ZJI winters, consistent with the merged jet structure.

5 Connection to Atlantic SST

The winter of 2010 was also characterized by strong North Atlantic SST anomalies (Taws et al., 2011; Buchan et al., 2014, and Fig. 7f). Fig. 10a,b shows the composites of SST anomalies and

²We note that 1996 and 2005 were chosen since their ZJI values were the most negative, however, these may not be the most optimal years for detecting a tropical Pacific role since their TPAI values were positive. An examination of the winter of 2010 back trajectories separately from the winters of 1996 and 2005 shows an increase in the number of trajectories coming from the tropical Pacific, but this increase was larger during 2010, in particular in the western part (between $120^{\circ}E - 150^{\circ}W$).

309 their meridional gradients in the North Atlantic region, for the anomalously negative ZJI winter
310 months, using monthly ERSST data (Smith and Lawrimore, 2008) ranging from 1949-2012. We
311 also show the line of peak positive lower level wind anomalies (thick black line in Fig. 10a,b),
312 calculated from the negative ZJI composite of 925 – 700 *hPa* zonal wind anomalies³. We see
313 a significant North Atlantic tripole anomaly, with warm SSTs in the tropics and just south of
314 Greenland and cold water in between, with the line of maximum lower level westerlies slightly
315 equatorwards of the peak cold SST anomalies. This SST anomaly pattern is quite typical of
316 the ocean response during negative NAO conditions (e.g. Visbeck et al., 2003). The tropical
317 warm anomaly extends from the Eastern Tropical Atlantic, where variability was found to be
318 strongly correlated to ENSO (Enfield and Mayer, 1997), all the way to the western coast of Africa.
319 The meridional SST gradients are enhanced (more negative) in the subtropics (Figs. 10b). In the
320 Eastern Atlantic, the anomalous negative gradients coincide with the line of maximum anomalous
321 lower level westerlies, suggesting there is a possible positive SST-wind feedback in this region.
322 The SST anomalies last more than a month, with the high latitude and midlatitude anomalies
323 starting to diminish at lag 2 months and the subtropical warm anomaly lasting even 3 months
324 (not shown). While the SST anomaly pattern is quite typical of negative NAO conditions (e.g.
325 Visbeck et al., 2003), a closer examination shows that during the more persistent negative ZJI
326 winters, the SST gradients in the Eastern Subtropical Atlantic are anomalous even with respect
327 to typical negative NAO conditions. Fig. 10c shows the winter mean time series of the anomalous
328 meridional SST gradients averaged over a box in the Eastern subtropical Atlantic (20W – 50W,
329 24N – 34N, the blue box marked on Fig. 10b), in the region where the SST gradients are aligned
330 with the anomalous strong surface winds. We see two pairs of consecutive winters with very
331 negative gradients - 2010/2011 and 1969/1970 in which negative gradients are stronger during

³The 10 *m* wind anomalies give similar results.

332 the first winter. Taws et al. (2011) showed using subsurface ocean data that the SST anomalies
333 during 2010 were strong enough to affect the more persistent subsurface ocean and reemerge the
334 following winter. They further suggested that this reemergence contributed to the anomalously
335 negative NAO during early winter 2011. Though we do not have early subsurface observations,
336 the time series suggest this reemergence mechanism could also have occurred during 1969 and
337 1970, with the anomalous SST contributing to the anomalous jet state during the winter of 1970.
338 Examining the winter-mean ZJI time series (Fig. 4b), we see that indeed these winters were all
339 characterized by a negative ZJI (though in 2011 it lasted only during Nov-Dec). Moreover, we
340 see a clear coincidence between negative winter mean ZJI and strongly negative winter mean SST
341 gradient index (e.g winters of 1964, 1969, 1970, 1996, 2010). This suggests that anomalously
342 persistent zonal wind anomalies during zonal jet years acts to induce large Eastern Subtropical
343 Atlantic SST anomalies. These large SST anomalies, in turn, could also strengthen the wind
344 anomalies (c.f. Nakamura et al., 2004, 2008). While more studies need to be done to establish it, a
345 positive SST-jet feedback could explain the strong persistence of the zonal mean wind anomalies
346 during some of the negative ZJI episodes. Recently, Buchan et al. (2014) examined the role of
347 Atlantic SST anomalies in forcing the negative NAO during winters 2010 and early winter 2011
348 using a coupled GCM, and found a significant role only for the early winter 2011. They however
349 emphasized the role of SSTs in initiating the negative NAO conditions, and did not examine
350 their role in increasing NAO persistence, thus their results are not inconsistent with our findings.

351 **6 Connection of ZJI to other atmospheric indexes**

352 The results of previous sections suggest El Nino conditions contributed to the onset of the
353 anomalously zonal jet state, by strengthening the thermal forcing of the jet. We also saw a

354 strong resemblance of negative ZJI months to a negative NAO state. In this section we examine
355 the statistical relation between the ZJI, the NAO index and ENSO. Fig. 11 shows a scatter plot
356 of monthly Nino 3.4 index values with the colors marking the NAO index (negative NAO in blue
357 and positive in red). We see that except for one month, jets with a strongly negative ZJI are in
358 a negative NAO state, while positive ZJI months occur more with a positive NAO. This explains
359 the similarity between the negative ZJI composites and NAO composites. On the other hand,
360 not all negative NAO states are characterized by a zonal jet.

361 We also see that with the exception of one month, anomalously zonal jets (ZJI smaller than
362 $-1std$) have not occurred during a strong a Nina, suggesting La nina conditions are detrimental
363 to the merging of the Atlantic and African jets. This is consistent with the notion that the
364 merging of these jets is due to the eddy and thermal jet forcings both playing a role in forcing
365 the jet during these years. The relation between ENSO and the ZJI, however, is complex.
366 In particular, it seems to be different during positive and negative NAO months, with ENSO
367 and ZJI being slightly positively correlated during positive NAO months (correlation of 0.17,
368 92% significance), and slightly (but not significantly) correlated during negative NAO months
369 (correlation of -0.96). This is consistent with the picture that under the right conditions of weak
370 enough eddies which have not shifted the jet too far poleward (a negative NAO), tropical heating
371 during can zonalize the Atlantic jet by inducing a merged thermally/eddy-driven jet state.

372 **7 Summary and conclusion**

373 We have shown that the Northern winter of 2010 (Dec 2009 - Mar 2010) was characterized by
374 an anomalously zonal jet, in which the Atlantic jet shifted slightly southward and assumed a
375 more zonal position, while the African subtropical jet shifted slightly poleward so that the two

376 jets connected to form one elongated zonal jet. Moreover, the latitude-height structure and
377 temporal variability of the Atlantic jet were more characteristic of the Pacific than the Atlantic
378 during this winter. In the context of characterizing the jet stream types (e.g. Son and Lee,
379 2005), it seems that during this winter, the jet changed from being eddy-driven to being a mixed
380 eddy/thermally-driven jet. This paper examines the possible transition of the Atlantic jet stream
381 from an eddy-driven to a merged jet, as part of the large inter annual variability in the Atlantic.
382 We defined a Zonal Jet Index (ZJI) which characterizes the zonal gradient in the latitude of the
383 jet axis, with anomalously negative values representing anomalously zonal jets. Calculating this
384 index for monthly data allows us to identify zonal jet months. We find that while an unusually
385 zonal state occurs occasionally for a month, it is quite rare for it to be dominant for a whole
386 winter, with the last occurrence before 2010 being the winters of 1969 and 1970. A composite
387 analysis of various eddy quantities in comparison to the climatology shows a picture similar to a
388 negative NAO state, with eddies and eddy fluxes being weaker, and shifted anomalously south. A
389 composite analysis of various quantities related to diabatic heating, including total atmospheric
390 column heating, precipitation, vertical velocities and anomalous SSTs, show anomalous heating
391 in the tropical Pacific. This suggests the combination of weaker eddies and enhanced tropical
392 heating, with positive eddy-mean flow feedbacks, push the jet from being eddy-driven to being
393 partly thermally-driven as in the Pacific (Li and Wettstein, 2012). A Lagrangian back-trajectory
394 analysis of the African and Atlantic jets shows that indeed the tropical Pacific is one of the
395 sources of momentum for both jets, and that during negative ZJI years this source is enhanced
396 relative to other years.

397 A composite of SST anomalies shows a typical Atlantic tripole pattern (with a phase charac-
398 teristic of a negative NAO pattern) but with particularly anomalous meridional gradients in the
399 eastern subtropical Atlantic, where the surface wind is anomalously westerly. Previous studies

400 found a strong SST feedback over the Gulf stream region (e.g. Ciasto and Thompson, 2004). We
401 find that when the anomalous meridional gradients become negative enough in the Eastern sub-
402 tropical Atlantic, an anomalously zonal jet state persists, suggesting a positive SST feedback, but
403 in the Eastern subtropical and mid-latitude Atlantic. Moreover, the SST gradient anomalies in
404 the observational record appeared in pairs of two consecutive winters: 1969/1970 and 2010/2011,
405 with the earlier winters showing stronger anomalies, suggesting these strong anomalies reach the
406 deep waters and reemerge to strengthen the zonal jet state during the following winter (as in
407 Taws et al., 2011).

408 Thus the picture which emerges is that the Atlantic jet undergoes typical variations associated
409 with eddy-mean flow interactions, which give rise to the typical Atlantic variability associated
410 with the NAO. During a few winters when an anomalously equatorwards jet coincides with
411 anomalous tropical heating, the jet can undergo a transition to a mixed thermally/eddy-driven
412 jet state, which is more characteristic of the Pacific. Woollings et al. (2010b) examined the
413 distribution of NAO phases, and attributed the observed skewness to the existence of two different
414 flow regimes- a “Greenland Blocking” pattern more characteristic of a negative NAO, and a “sub-
415 polar jet” state more characteristic of a positive NAO, each of which exhibits variability with a
416 Gaussian distribution. The relation between Greenland Blocking and the type of jet stream is
417 left for a future study.

418 *Acknowledgments* We acknowledge support received by a the Israeli Science Foundation grants
419 1370/08 and 1537/12. O. Adam acknowledges an Israeli Vatat postdoctoral grant. GPCP
420 Precipitation data was provided by the NOAA/OAR/ESRL PSD, Boulder, Colorado, USA,
421 from their Web site at <http://www.esrl.noaa.gov/psd/>. We thank Eyal Heifetz for insightful
422 discussions. Most of the calculations presented here were performed using GOAT (Geophysical
423 Observation Analysis Tool), a freely available MATLAB based tool for management, analysis

424 and visualization of geophysical data (<http://www.goat-geo.org>).

425 **References**

- 426 Adler, R. F. et al., 2003: The version 2 global precipitation climatology project (GPCP) monthly
427 precipitation analysis (1979-present), *J. Hydrometeor.*, **4**, 1147–1167.
- 428 Barnston, R. E. L., Anthony G., 1987: Classification, seasonality and persistence of low-frequency
429 atmospheric circulation patterns, *Mon. Wea. Rev.*, **115**, 1083–1126.
- 430 Bordoni, S. and T. Schneider, 2010: Regime transitions of steady and time-dependent hadley
431 circulations: Comparisons of axisymmetric and eddy-permitting simulations, *J. Atmos. Sci.*,
432 **67**, 1643–1654.
- 433 Buchan, J., J. J.-M. Hirschi, A. T. Blaker, and B. Sinha, 2014: North Atlantic SST anomalies
434 and the cold North European weather events of winter 2009/10 and december 2010, *Mon.*
435 *Wea. Rev.*, **142**, 922–932.
- 436 Cattiaux, J., R. Vautard, C. Cassou, P. Yiou, V. Masson-Delmotte, and F. Codron, 2010:
437 Winter 2010 in europe: A cold extreme in a warming climate, *Geophys. Res. Lett.*, **37**(20),
438 10.1029/2010GL044613.
- 439 Ciasto, L. M. and D. W. Thompson, 2004: North atlantic atmosphere-ocean interaction on
440 intraseasonal time scales, *J. Clim.*, **17**(8), 1617–1621.
- 441 Dee, D. P. et al., 2011: The ERA-Interim reanalysis: configuration and performance of the data
442 assimilation system., *Q. J. R. Meteorol. Soc.*, **137**, 553–597.
- 443 Eichelberger, S. J. and D. L. Hartmann, 2007: Zonal jet structure and the leading mode of
444 variability, *J. Clim.*, p. 5149–5163.

445 Enfield, D. B. and D. A. Mayer, 1997: Tropical atlantic sea surface temperature variability and
446 its relation to el nio-southern oscillation, *J. Geophys. Res.: Oceans*, **102**, 929–945.

447 Held, I. M., 1975: Momentum transport by quasi-geostrophic eddies., *J. Atmos. Sci.*, **32**, 1494–
448 1497.

449 Held, I. M., 2000: The general circulation of the atmosphere. introduc tion to gen-
450 eral circulation theories., *Proc. Prog. Geophys. Fluid Dyn. Woods Hole Oceanogr. Inst.*,
451 <http://gfd.whoi.edu/proceedings/2000/PDFvol2000.html>.

452 Held, I. M. and A. Y. Hou, 1980: Nonlinear axially symmetric circulations in a nearly inviscid
453 atmosphere, *J. Atmos. Sci.*, **37**(3), 515–533.

454 Kalnay, E. et al., 1996: The NCEP/NCAR 40-year reanalysis project, *B. Am. Meteorol. Soc.*,
455 **77**(434-471).

456 Koch, P., H. Wernli, and H. C. Davies, 2006: An event-based jet-stream climatology and typol-
457 ogy., *Int. J. Climatol.*, (26), 283–301.

458 Lachmy, O. and N. Harnik, 2014: The transition to a subtropical jet regime and its maintenance,
459 *J. Atmos. Sci.*, **71**, 1389–1409.

460 Lee, S. and H. K. Kim, 2003: The dynamical relationship between subtropical and eddy-driven
461 jets, *J. Atmos. Sci.*, **60**, 1490–1503.

462 Li, C. and J. J. Wettstein, 2012: Thermally driven and eddy-driven jet variability in reanalysis,
463 *J. Clim.*, p. 15871596.

464 Martius, O., 2014: A lagrangian analysis of the northern hemisphere subtropical jet, *J. Atmos.*
465 *Sci.*, **71**, in press.

466 Martius, O. C. and H. Wernli, 2012: A trajectory-based investigation of physical and dynamical
467 processes that govern the temporal evolution of the subtropical jet streams over africa, *J.*
468 *Atmos. Sci.*, **69**, 1602–1616.

469 Nakamura, H. and T. Sampe, 2002: Trapping of synoptic-scale disturbances into the north-pacific
470 subtropical jet core in midwinter, *Geophys. Res. Lett.*, **29**(16), art. no.–1761.

471 Nakamura, H., T. Sampe, A. Goto, W. Ohfuchi, and S.-P. Xie, 2008: On the importance of mid-
472 latitude oceanic frontal zones for the mean state and dominant variability in the tropospheric
473 circulation, *Geophys. Res. Lett.*, **35**(15).

474 Nakamura, H., T. Sampe, Y. Tanimoto, and A. Shimpo, 2004: Observed associations among
475 storm tracks, jet streams and midlatitude oceanic fronts, *Geophysical Monograph Series*, **147**,
476 329–345.

477 O’Rourke, A. and G. K. Vallis, 2013: Jet interaction and the influence of a minimum phase speed
478 bound on the propagation of eddies, *J. Atmos. Sci.*, **70**, 2614–2628.

479 Panetta, R. L., 1993: Zonal jets in wide baroclinically unstable regions: Persistence and scale
480 selection, *J. Atmos. Sci.*, **50**, 2073–2106.

481 Rhines, P. B., 1975: Waves and turbulence on a beta-plane, *J. Fluid Mech.*, **69**, 417–443.

482 Romanski, W. B. R., Joy, 2013: Contributions of individual atmospheric diabatic heating pro-
483 cesses to the generation of available potential energy, *J. Clim.*, **26**, 42444263.

484 Santos, J., T. Woollings, and J. Pinto, 2013: Are the winters 2010 and 2013 archetypes exhibiting
485 extreme opposite behavior of the north atlantic jet stream?, *Mon. Wea. Rev.*, **141**, 3626–3640.

486 Schneider, E. K., 1977: Axially symmetric steady-state models of the basic state for instability
487 and climate studies. part II. nonlinear circulations, *J. Atmos. Sci.*, **34**, 280–296.

488 Seager, R., Y. Kushnir, J. Nakamura, M. Ting, and N. Naik, 2010: Northern hemisphere
489 winter snow anomalies: Enso, nao and the winter of 2009/10, *Geophys. Res. Lett.*, **37**,
490 10.1029/2010GL043830.

491 Smith, R. R. T. C. P., T.M. and J. Lawrimore, 2008: Improvements to noaa’s historical merged
492 land-ocean surface temperature analysis (1880-2006), *J. Clim.*, **21**, 2283–2296.

493 Smith, T. and R. Reynolds, 2004: Improved extended reconstruction of SST (1854-1997), *J.*
494 *Clim.*, **17**, 2466–2477.

495 Son, S. W. and S. Lee, 2005: The response of westerly jets to thermal driving in a primitive
496 equation model, *J. Atmos. Sci.*, **62**, 3741–3757.

497 Taws, S. L., R. Marsh, N. C. Wells, and J. Hirschi, 2011: Re-emerging ocean temperature
498 anomalies in late-2010 associated with a repeat negative NAO, *Geophys. Res. Lett.*, **38**,
499 10.1029/2011GL048978.

500 Trenberth, K. E. and A. Solomon, 1994: The global heat balance: Heat transports in the atmo-
501 sphere and ocean, *Clim. Dyn.*, **10**, 107–134.

502 Uppala, S. M. et al., 2005: The ERA-40 re-analysis., *Q. J. R. Meteorol. Soc.*, **131**, 2961–3012.

503 Vincente-Serrano, S. M., R. M. Trigo, J. I. Lopez-Moreno, M. L. R. Liberato, et al., 2011: Extreme
504 winter precipitation in the iberian peninsula in 2010: anomalies, driving mechanisms and future
505 projections, *Clim. Res.*, **46**, 51–65.

506 Visbeck, M., E. P. Chassignet, R. G. Curry, T. L. Delworth, R. R. Dickson, and G. Krahnmann,
507 2003: The ocean’s response to north atlantic oscillation variability, *The North Atlantic Oscil-*
508 *lation: climatic significance and environmental impact*, pp. 113–145.

- 509 Wang, C., H. Liu, and S.-K. Lee, 2010: The record-breaking cold temperatures during the
510 winter of 2009/2010 in the northern hemisphere, *Atmospheric Science Letters*, **11**, 161–168,
511 10.1002/asl.278.
- 512 Woollings, T., A. Hannachi, and B. Hoskins, 2010a: Variability of the north atlantic eddy-driven
513 jet stream, *Q. J. R. Meteorol. Soc.*, **136**, 856–868.
- 514 Woollings, T., A. Hannachi, B. Hoskins, and A. Turner, 2010b: A regime view of the north
515 atlantic oscillation and its response to anthropogenic forcing, *J. Clim.*, **23**(6), 1291–1307.

516 **Figure captions**

517 Fig. 1. 300 *hPa* zonal wind: a) Dec 2009 - Mar 2010 mean. b) Dec-Mar climatology (1949-2012).
518 c,d) as in a,b) but for 925 – 700 *hPa*. The jet axis (latitude of maximum zonal wind) is marked
519 by the thick black lines. Contour intervals are 10*m/sec* and 3*m/sec* for the upper and lower
520 level winds, respectively. In plots (a)(b) contour values of 10*m/sec* and less are dashed, while in
521 plots (c)(d) values of 3*m/sec* and lower are dashed.

522

523 Fig. 2. Latitude-height plots of the Dec-Mar mean zonal wind. a) Climatological values, av-
524 eraged zonally over the Pacific (120W-120E). b) Climatological values, averaged zonally over
525 the Atlantic (100W-0E). c) Dec 2009-Mar 2010 mean over the Atlantic (100W-0E). The contour
526 interval is 5*m/sec*, zero line is marked by a thick line, and negative values are dashed.

527

528 Fig. 3. Top) Latitude-year plots of the winter mean (Dec - Mar) 300 *hPa* zonal wind, averaged
529 over the Pacific region (120W-120E average); Middle) As in the top plot but for the Atlantic
530 region (100W-0E average); Bottom) Day-latitude plot of 300 *hPa* zonal wind in the Atlantic
531 region (100W-0E), for the period of Dec 1 2009 - Mar 31 2010.

532

533 Fig. 4. Time series of the Zonal Jet Index (ZJI), based on monthly (top) and winter (Dec-Mar
534 mean, bottom) 300 *hPa* zonal winds. The dashed lines mark the 1 standard deviation line (the
535 mean is zero by construction), based on the monthly data. In the top graph, all months are
536 shown and those Dec-March months with an anomaly larger than one standard deviation (of
537 either sign) are marked with circles.

538

539 Fig. 5. Composites for anomalously zonal jet months (anomalously negative ZJI) of a) 300 *hPa*

540 U, b) 300 *hPa* U anomaly (the deviation from the climatological seasonal cycle). c) As in (a) but
 541 for months with anomalously positive ZJI values. d) As in (a) but for months with an anoma-
 542 lously negative NAO phase. Shading represents regions for which the composites are significant
 543 at 99.9% based on a two sided T-test against climatology. In plots (a,c,d) contour interval is
 544 5*m/sec* and values of 20*m/sec* or smaller are dashed. In plot (b) contour interval is 3*m/sec*,
 545 negative values are dashed and the zero line is thick.

546

547 Fig. 6. a)-c) 300 *hPa* eddy v variance $\langle v'^2 \rangle$, with ($'$) denoting a 10-day high passed field, and
 548 $\langle () \rangle$ denoting the 10 day low passed field): a) Dec-Mar climatology. b)-c) The composite of
 549 negative ZJI Dec-Mar months, of the total field (b) and its anomaly with respect to the clima-
 550 tological seasonal cycle (c). d) As in c) but for 850 – 600 *hPa* mean $\langle v'T' \rangle$ anomaly e) As in
 551 c) but for 300 *hPa* eddy $\langle u'v' \rangle$ anomaly. f) as in c) but for the meridional eddy momentum
 552 flux convergence (cosine squared weighted meridional gradient of $\langle u'v' \rangle$). The Shading repre-
 553 sents regions for which the composites are significant at the 99% value. Contour intervals: a)-b)
 554 25*m²/sec²* in , values of 75*m²/sec²* and less are dashed. c) 15*m²/sec²*, d) 2*Km/sec* with $\pm 1K$
 555 contour added, e) 5*m²/sec²*, f) $2 \times 10^{-5}K/sec$. In c)-f) negative values are dashed. All fields
 556 calculated using NCEP reanalysis from 1948-2012.

557

558 Fig. 7. Negative ZJI composites of monthly anomalies of the following fields a)-d) Era Interim
 559 diabatic heating (1979-2012). b) NCEP reanalysis diabatic heating (2002-2012) c) GPCP precip-
 560 itation rate (1979-2012). d-e) NCEP 600 – 400 *hPa* mean vertical pressure velocity ω (1949-2012,
 561 negative values in solid), for time lags 0, -2 months. f) SST anomaly (1949-2012). Contour in-
 562 tervals are: Diabatic heating - 30*W/m²*. Precipitation - 1*mm/day*. Vertical pressure velocity -
 563 0.01 *hPa/sec*, with ± 0.005 *hPa/sec* contour added, SST - 0.15*K*. Negative values are dashed

564 except for vertical pressure velocity for which positive values are dashed. Zero contours are omit-
565 ted. Gray shadings represent 95% and 99% significance levels (darker marks higher significance).

566

567 Fig. 8. Negative ZJI composites of monthly anomalies of NCEP 600 – 400 *hPa* mean vertical
568 pressure velocity ω for subsets of the data used to create Fig. 7d: a) winters 1949-2011, with Dec
569 2009-Mar 2010 excluded. b) Winters 1979-2011, all months. c) Winters 1979-2011, excluding
570 Dec 2009 - Mar 2010. d) A scatterplot of the Dec-Mar TPAI vs ZJI values, with winter months
571 before Dec 1978 in red. The months of winter 2010 are also marked by large circles. For reference
572 we mark the minus 1 standard deviation of ZJI by a dashed black line.

573

574 Fig. 9. A 168 hour back-trajectory analysis starting from the Eastern Atlantic (90W 45W, plots
575 a,c,e) and African (30W 30E, plots b,d,f) subtropical jet regions. Shown is the fraction of the
576 total number of trajectories which cross each grid point over the entire seven day period, aver-
577 aged over the negative ZJI winters of 1996, 2005, 2010 (plots a,b) and the five winters of 1997
578 and 2006-9 (plots c,d). The bold contours correspond to a fraction 5×10^{-5} on the day when
579 the trajectories are started and they roughly indicate the starting regions. Plots e,f show the
580 difference between the negative ZJI winters (1996, 2005, 2010) minus 1997 and 2006-9, for the
581 Atlantic and African jets respectively.

582 Fig. 10. The negative ZJI composites of a) SST anomalies and b) meridional gradients of the
583 SST anomaly. Also shown in plots a-b is the line of maximum positive lower level (925 – 700 *hPa*
584 mean) wind anomalies. c) The Dec-Mar mean meridional SST gradients, averaged over 24–34°N,
585 50 – 20°W. Dashed lines mark \pm 1std. In the composite plots, the light and dark gray shadings
586 respectively mark the 95% and 99% significance regions, negative values dashed and the zero
587 contour omitted. Contour interval is 0.15K for SST and $3 \cdot 10^{-7} K/m$ for SST gradients.

588

589 Fig. 11. Scatter plot of the monthly Nino 3.4 index, vs the Zonal Jet index. Colors mark the
590 normalized NAO index value with negative NAO in blue and positive in red. Large circles show
591 Dec 2009 - Mar 2010. Anomalously zonal jet months have ZJI values smaller than $-1std$ -
592 marked by the vertical black line. $\pm 1std$ lines of the Nino3.4 index are marked by the horizontal
593 black lines.

594

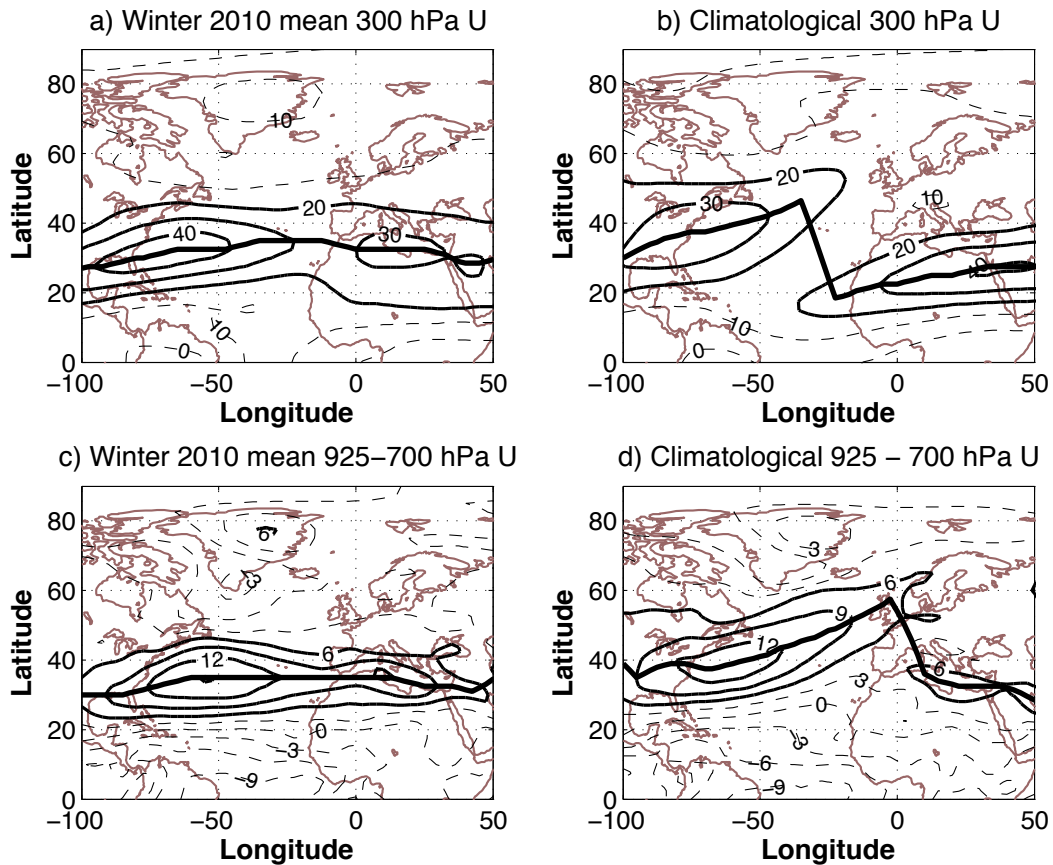


Figure 1: 300 *hPa* zonal wind: a) Dec 2009 - Mar 2010 mean. b) Dec-Mar climatology (1949-2012). c,d) as in a,b) but for 925 – 700 *hPa*. The jet axis (latitude of maximum zonal wind) is marked by the thick black lines. Contour intervals are 10*m/sec* and 3*m/sec* for the upper and lower level winds, respectively. In plots (a)(b) contour values of 10*m/sec* and less are dashed, while in plots (c)(d) values of 3*m/sec* and lower are dashed.

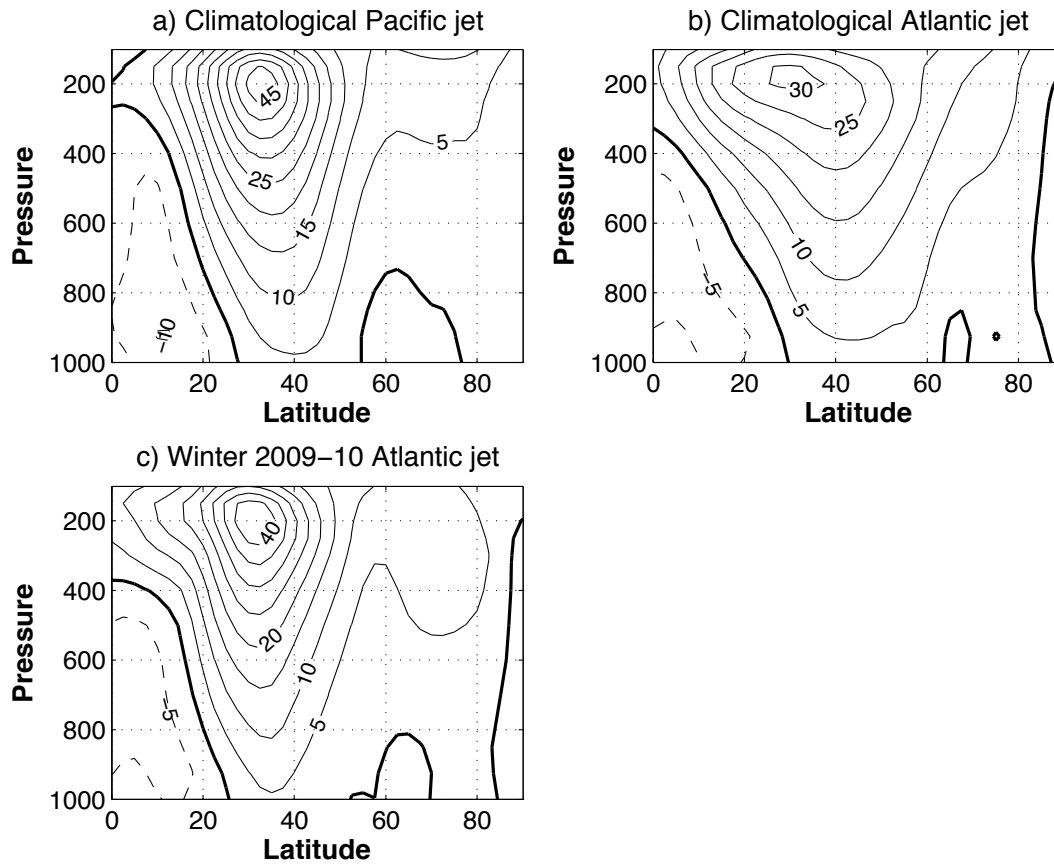


Figure 2: Latitude-height plots of the Dec-Mar mean zonal wind. a) Climatological values, averaged zonally over the Pacific (120W-120E). b) Climatological values, averaged zonally over the Atlantic (100W-0E). c) Dec 2009-Mar 2010 mean over the Atlantic (100W-0E). The contour interval is 5m/sec, zero line is marked by a thick line, and negative values are dashed.

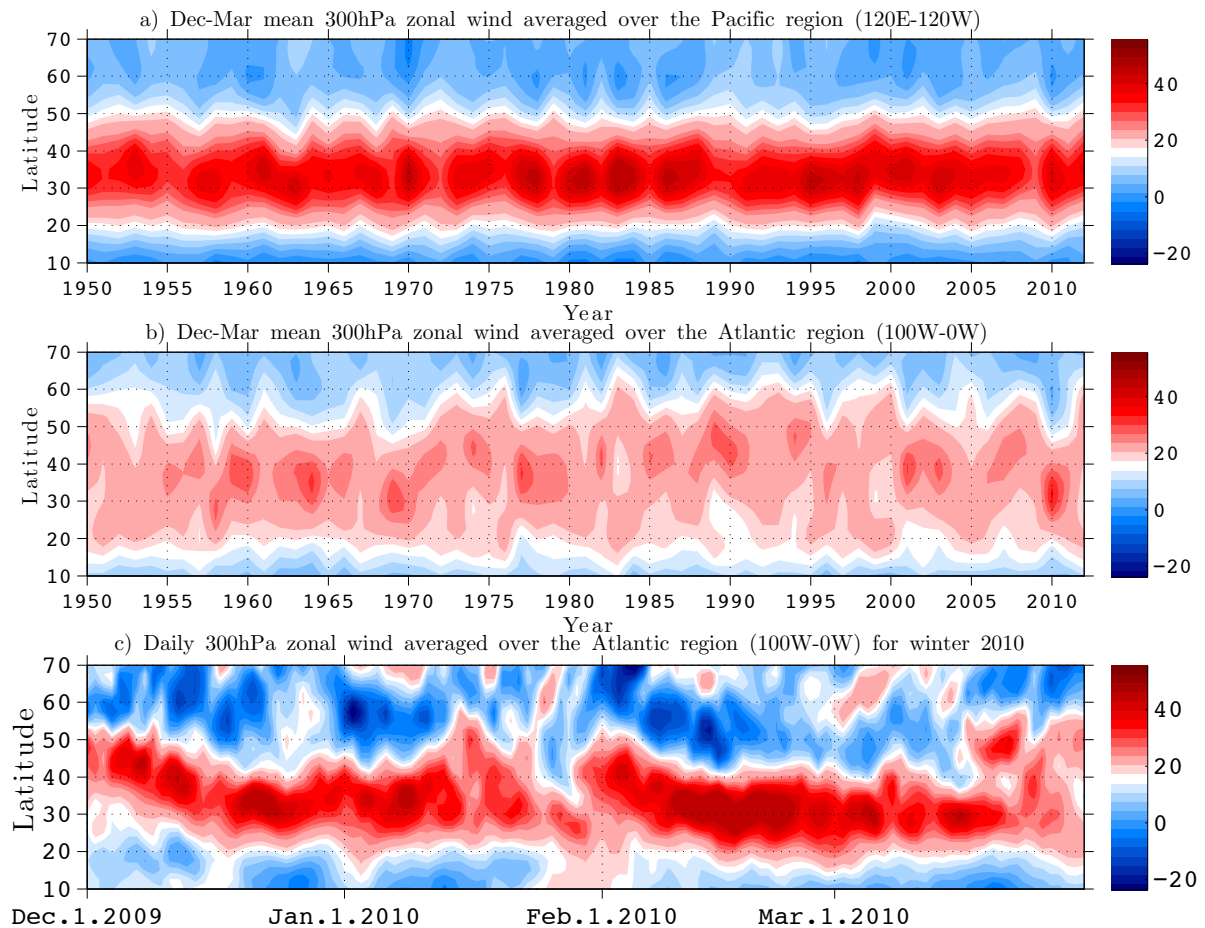


Figure 3: Top) Latitude-year plots of the winter mean (Dec - Mar) 300 *hPa* zonal wind, averaged over the Pacific region (120W-120E average); Middle) As in the top plot but for the Atlantic region (100W-0E average); Bottom) Day-latitude plot of 300 *hPa* zonal wind in the Atlantic region (100W-0E), for the period of Dec 1 2009 - Mar 31 2010.

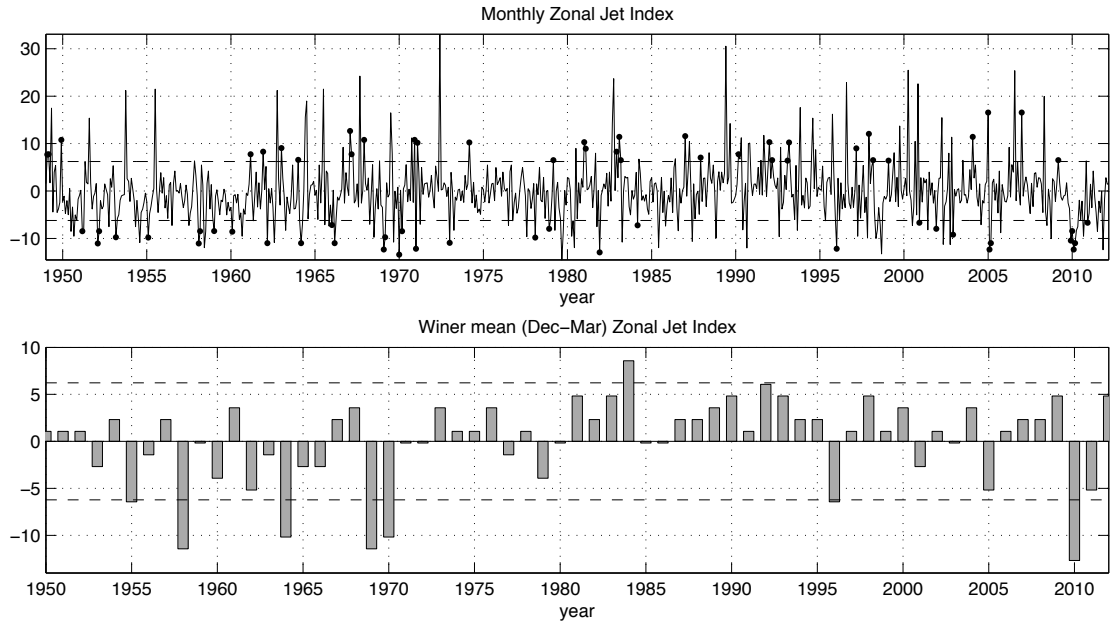


Figure 4: Time series of the Zonal Jet Index (ZJI), based on monthly (top) and winter (Dec-Mar mean, bottom) 300 hPa zonal winds. The dashed lines mark the 1 standard deviation line (the mean is zero by construction), based on the monthly data. In the top graph, all months are shown and those Dec-March months with an anomaly larger than one standard deviation (of either sign) are marked with circles.

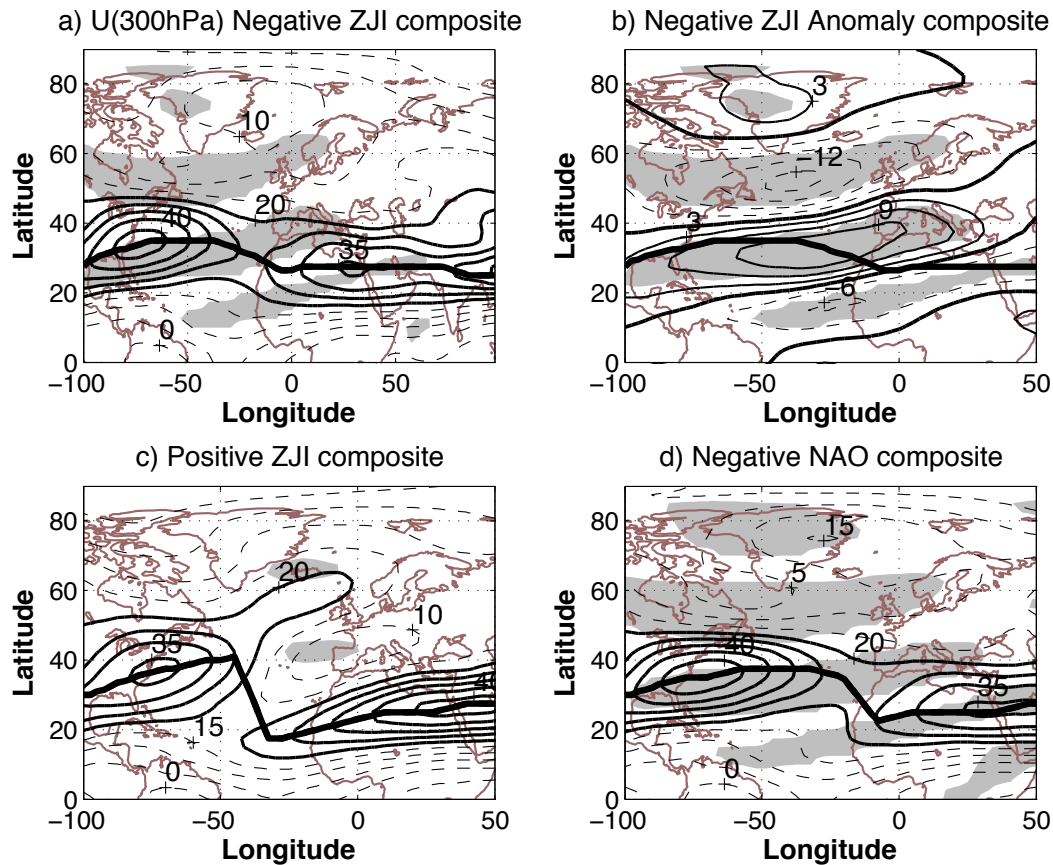


Figure 5: Composites for anomalously zonal jet months (anomalously negative ZJI) of a) 300 *hPa* U, b) 300 *hPa* U anomaly (the deviation from the climatological seasonal cycle). c) As in (a) but for months with anomalously positive ZJI values. d) As in (a) but for months with an anomalously negative NAO phase. Shading represents regions for which the composites are significant at 99.9% based on a two sided T-test against climatology. In plots (a,c,d) contour interval is 5*m/sec* and values of 20*m/sec* or smaller are dashed. In plot (b) contour interval is 3*m/sec*, negative values are dashed and the zero line is thick.

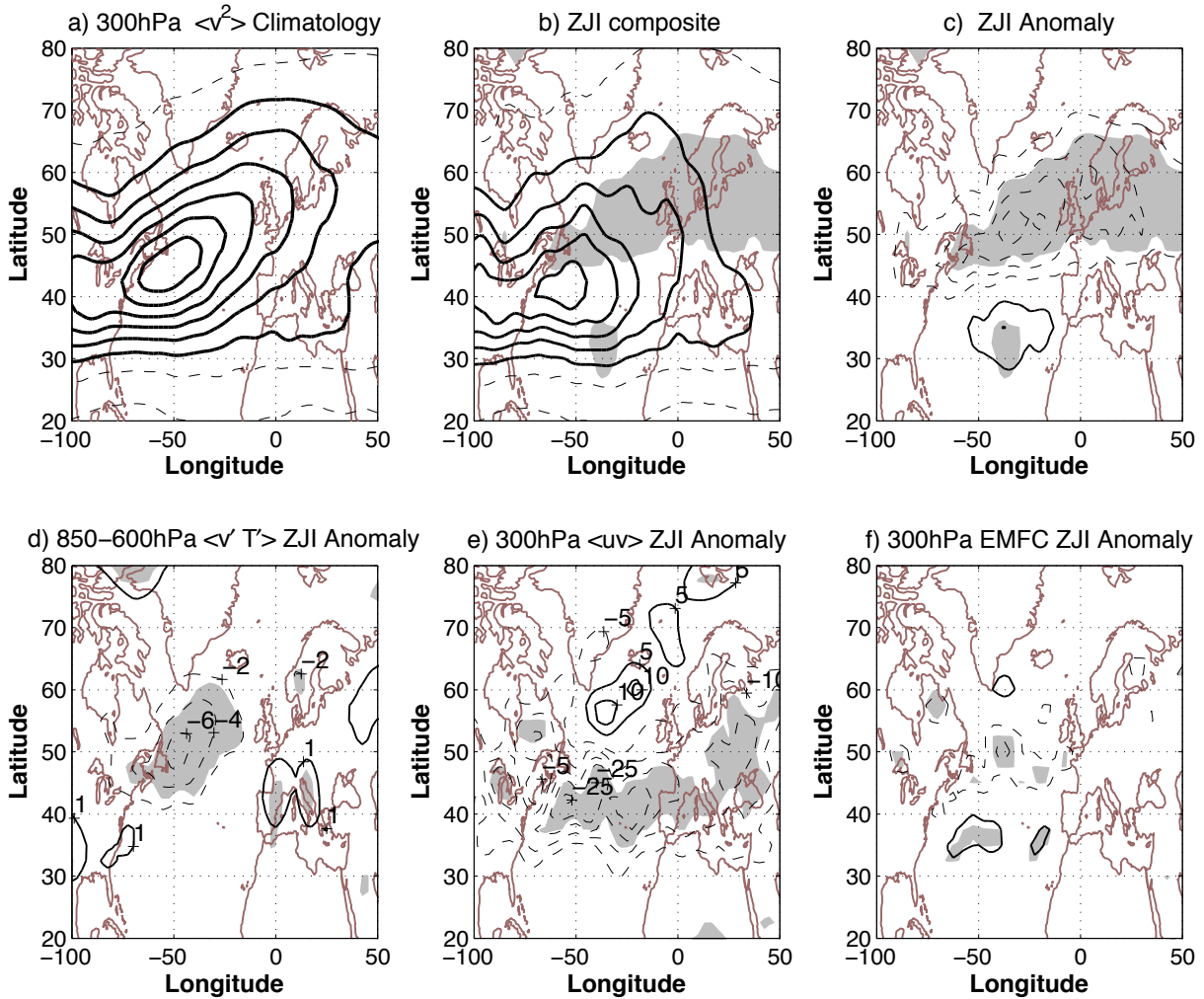


Figure 6: a)-c) 300 *hPa* eddy v variance $\langle v'^2 \rangle$, with $(')$ denoting a 10-day high passed field, and $\langle \rangle$ denoting the 10 day low passed field): a) Dec-Mar climatology. b)-c) The composite of negative ZJI Dec-Mar months, of the total field (b) and its anomaly with respect to the climatological seasonal cycle (c). d) As in c) but for 850 – 600 *hPa* mean $\langle v'T' \rangle$ anomaly e) As in c) but for 300 *hPa* eddy $\langle u'v' \rangle$ anomaly. f) as in c) but for the meridional eddy momentum flux convergence (cosine squared weighted meridional gradient of $\langle u'v' \rangle$). The Shading represents regions for which the composites are significant at the 99% value. Contour intervals: a)-b) $25m^2/sec^2$ in , values of $75m^2/sec^2$ and less are dashed. c) $15m^2/sec^2$, d) $2Km/sec$ with $\pm 1K$ contour added, e) $5m^2/sec^2$, f) $2 \times 10^{-5}K/sec$. In c)-f) negative values are dashed. All fields calculated using NCEP reanalysis from 1948-2012.

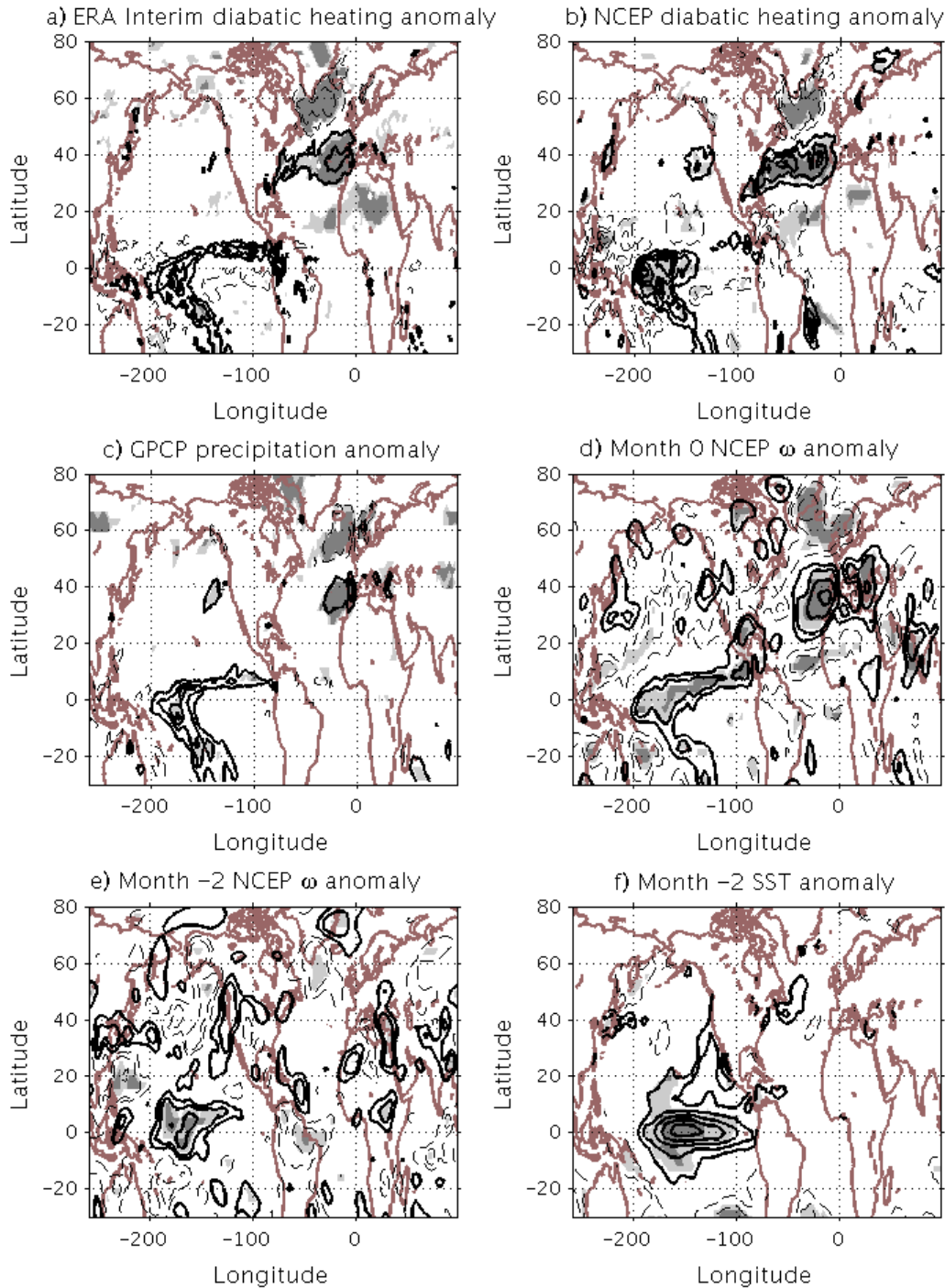


Figure 7: Negative ZJI composites of monthly anomalies of the following fields a)-d) Era Interim diabatic heating (1979-2012). b) NCEP reanalysis diabatic heating (2002-2012) c) GPCP precipitation rate (1979-2012). d-e) NCEP 600 – 400 hPa mean vertical pressure velocity ω (1949-2012, negative values in solid), for time lags 0, -2 months. f) SST anomaly (1949-2012). Contour intervals are: Diabatic heating - $30W/m^2$. Precipitation - $1mm/day$. Vertical pressure velocity - $0.01 hPa/sec$, with $\pm 0.005 hPa/sec$ contour added, SST - $0.15K$. Negative values are dashed except for vertical pressure velocity for which positive values are dashed. Zero contours are omitted. Gray shadings represent 95% and 99% significance levels (darker marks higher significance).

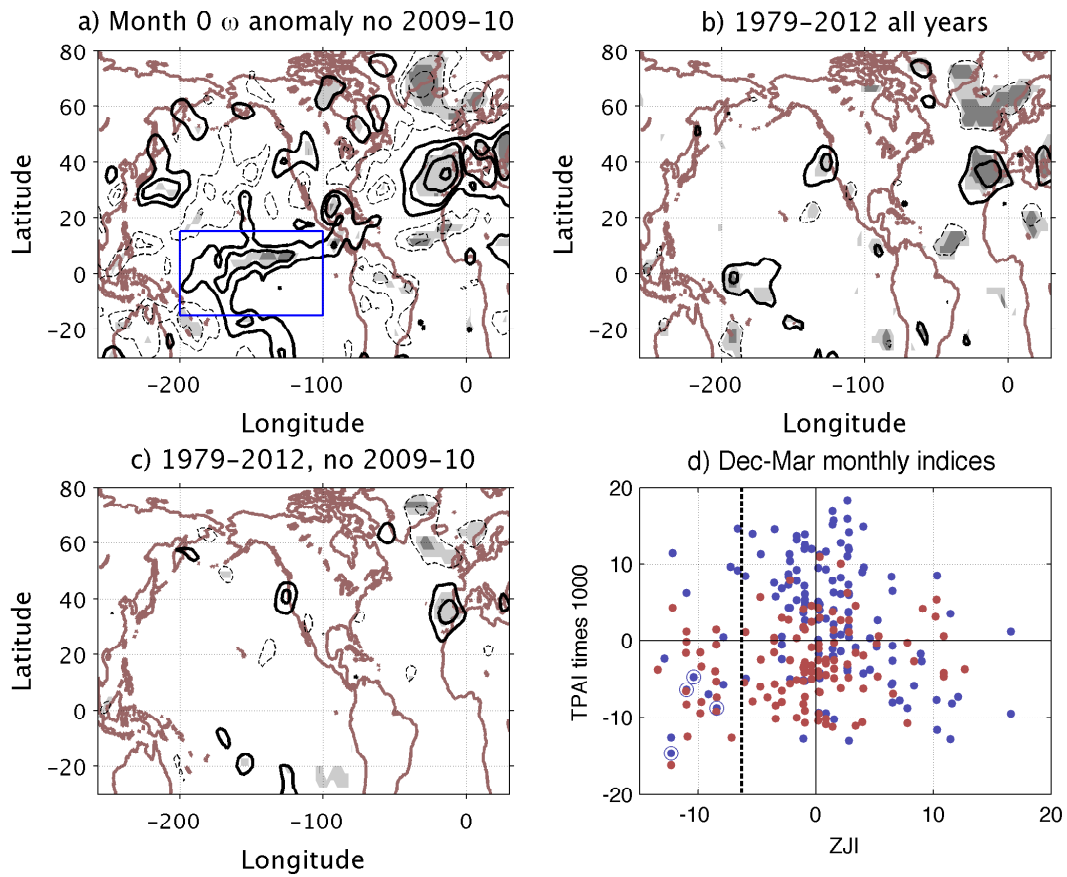


Figure 8: Negative ZJI composites of monthly anomalies of NCEP 600 – 400 hPa mean vertical pressure velocity ω for subsets of the data used to create Fig. 7d: a) winters 1949-2011, with Dec 2009-Mar 2010 excluded. b) Winters 1979-2011, all months. c) Winters 1979-2011, excluding Dec 2009 - Mar 2010. d) A scatterplot of the Dec-Mar TPAI vs ZJI values, with winter months before Dec 1978 in red. The months of winter 2010 are also marked by large circles. For reference we mark the minus 1 standard deviation of ZJI by a dashed black line.

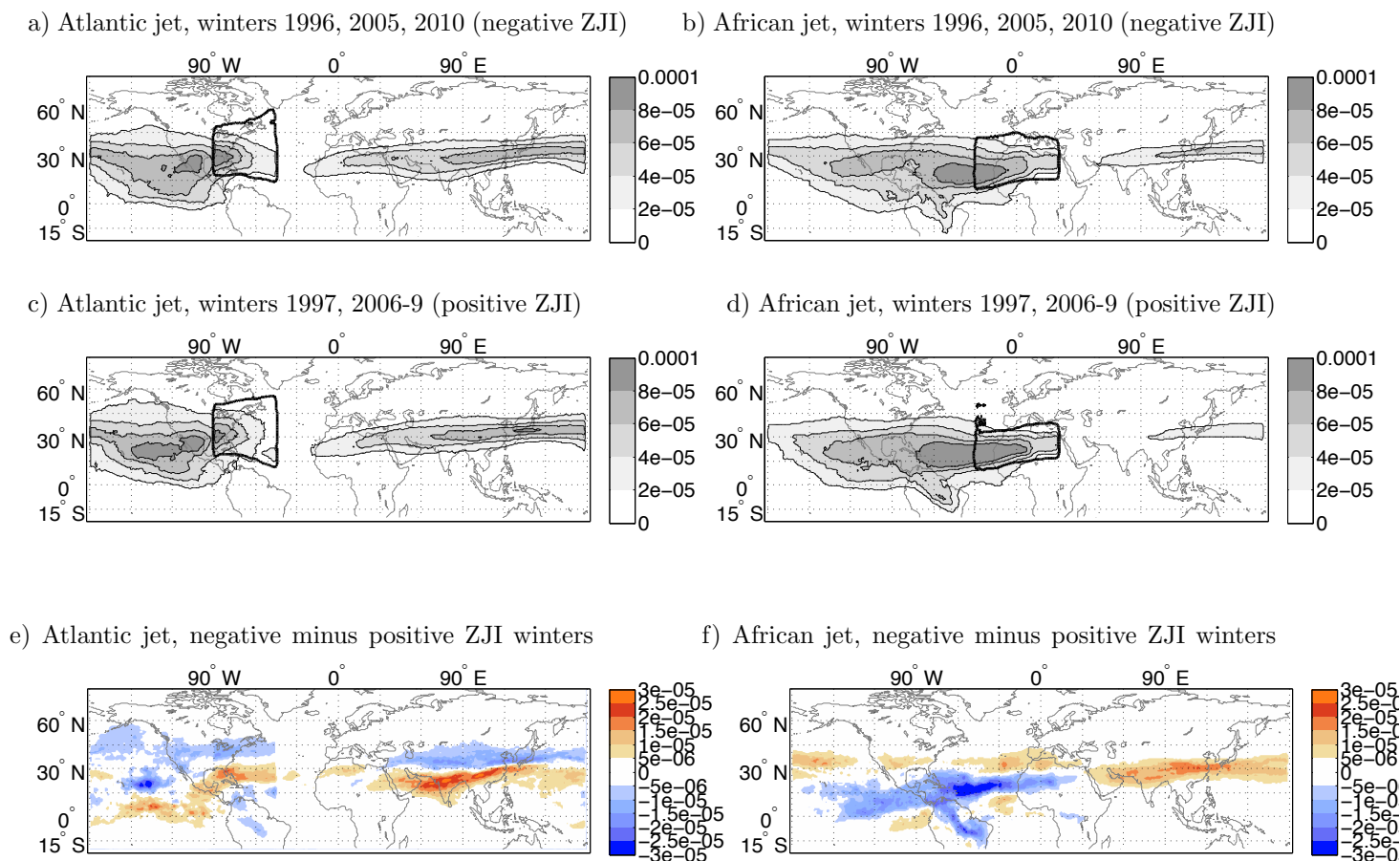


Figure 9: A 168 hour back-trajectory analysis starting from the Eastern Atlantic (90W 45W, plots a,c,e) and African (30W 30E, plots b,d,f) subtropical jet regions. Shown is the fraction of the total number of trajectories which cross each grid point over the entire seven day period, averaged over the negative ZJI winters of 1996, 2005, 2010 (plots a,b) and the five winters of 1997 and 2006-9 (plots c,d). The bold contours correspond to a fraction 5×10^{-5} on the day when the trajectories are started and they roughly indicate the starting regions. Plots e,f show the difference between the negative ZJI winters (1996, 2005, 2010) minus 1997 and 2006-9, for the Atlantic and African jets respectively.

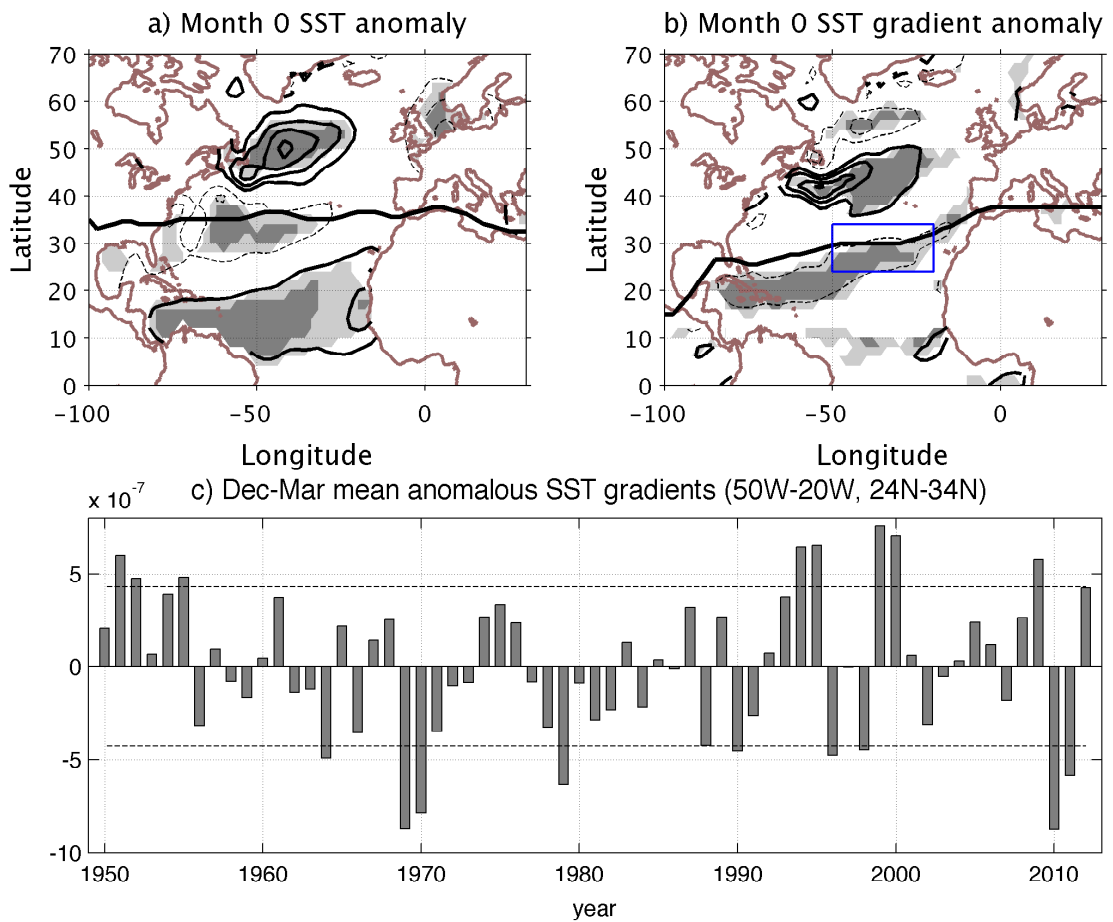


Figure 10: The negative ZJI composites of a) SST anomalies and b) meridional gradients of the SST anomaly. Also shown in plots a-b is the line of maximum positive lower level (925 – 700 hPa mean) wind anomalies. c) The Dec-Mar mean meridional SST gradients, averaged over 24–34°N, 50 – 20°W. Dashed lines mark ± 1 std. In the composite plots, the light and dark gray shadings respectively mark the 95% and 99% significance regions, negative values dashed and the zero contour omitted. Contour interval is $0.15K$ for SST and $3 \cdot 10^{-7} K/m$ for SST gradients.

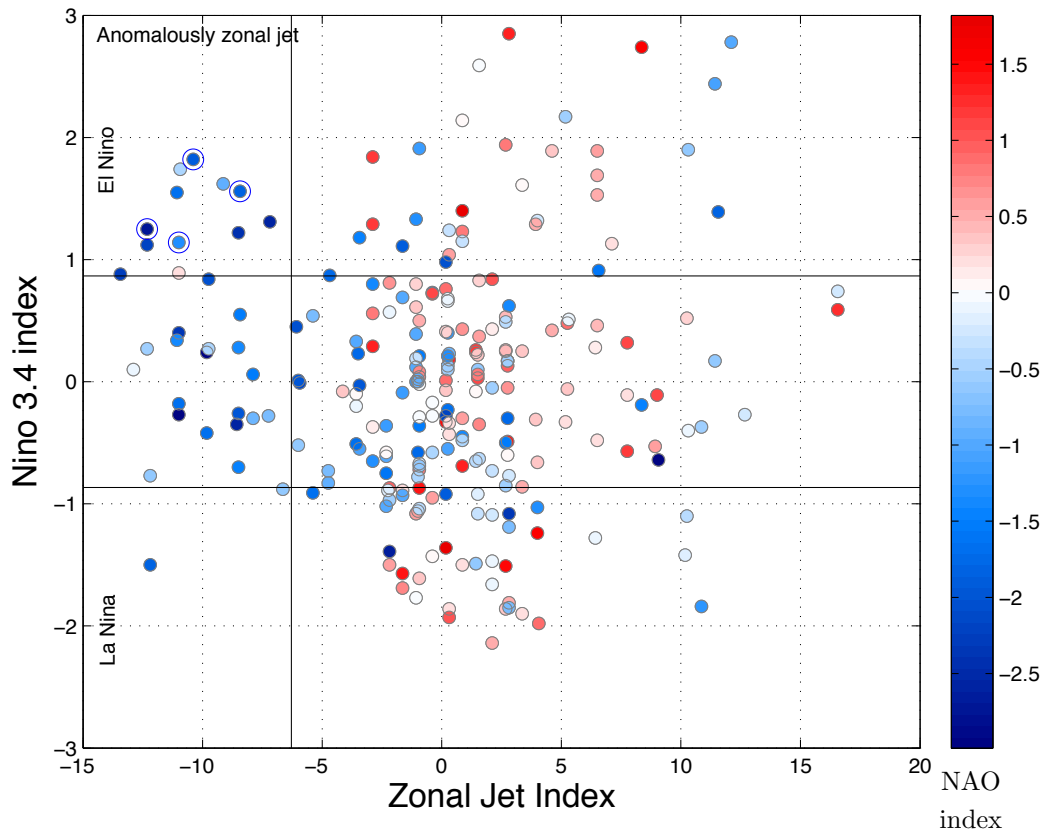


Figure 11: Scatter plot of the monthly Nino 3.4 index, vs the Zonal Jet index. Colors mark the normalized NAO index value with negative NAO in blue and positive in red. Large circles show Dec 2009 - Mar 2010. Anomalously zonal jet months have ZJI values smaller than $-1std$ - marked by the vertical black line. $\pm 1std$ lines of the Nino3.4 index are marked by the horizontal black lines.